Kubojima *et al. Journal of Wood Science* (2022) 68:39
https://doi.org/10.1186/s10086-022-02046-1

Journal of Wood Science

ORIGINAL ARTICLE Open Access

Application of a bending vibration method without weighing specimens to the practical wooden members conditions

Yoshitaka Kubojima[1*], Satomi Sonoda[2] and Hideo Kato[1]

Abstract

A vibration test to measure the mass of a specimen without weighing it using the difference between the resonance frequency with an additional mass and that without it (vibration method with additional mass, VAM) was applied to small, clear, and wooden specimens assuming practical situations. An apparatus that provided various end conditions by compressing the ends of the specimens was used in the tests. Bending vibration tests were performed on the specimens installed in the apparatus with/without an additional mass. Because the mass ratio (estimated mass by VAM/measured mass), namely, M_{VAM}/M_0, which represents the estimation accuracy of VAM, was stable when the compressive strength was sufficiently large, VAM could be adequately used when the specimen was properly installed in the apparatus. The end condition at maximum compressive stress by the apparatus was an imperfect fixed condition. The M_{VAM}/M_0 value greatly deviated from 1 in the specimens with a large height. The deviation in M_{VAM}/M_0 from 1 was due to the introduction of the measured resonance frequencies with/without a concentrated mass into the frequency equation that required resonance frequencies under an ideal fixed–fixed condition. A correction method for M_{VAM}/M_0 was then proposed.

Keywords: Additional mass, Fixed–fixed condition, Mass, Rotatory inertia, Semi-rigid, Shear, Vibration test

Introduction

Vibration test is a simple and nondestructive testing method for measuring the Young's modulus. Density is needed to calculate the Young's modulus. Weighing a specimen requires much time in some cases, such as weighing of each piled lumber and each round bar that is fixed to a post of a timber guardrail.

The mass of a specimen can be measured without weighing the specimen using the difference between the resonance frequency with an additional mass and that without it [1–5]. In the present study, this method is referred to as the "vibration method with additional mass (VAM)".

To analyze the potential practical application of VAM, a series of parameters was investigated, including the suitable mass ratio (additional mass/specimen) [6], connection between the additional mass and specimen [6], crossers' position of piled lumber [7], moisture content of specimen [8], bending vibration generation method [9], and effects of shear and rotatory inertia in bending [10]. VAM can be applied to a timber guardrail cross-beam [11], piled lumber [12], and piled round bars [13].

The end conditions of the specimens in the above-mentioned studies were simply supported, free, and fixed. However, the end conditions of actual wooden members do not represent these "ideal" conditions. For example, the end condition of a timber guardrail cross-beam is believed to be between the simply supported and fixed conditions, i.e., semi-rigid [14, 15]. Although the accurate mass of a timber guardrail cross-beam, which can reflect its deterioration, can be estimated

*Correspondence: kubojima@ffpri.affrc.go.jp

[1] Forestry and Forest Products Research Institute, 1 Matsunosato, Tsukuba, Ibaraki 305-8687, Japan
Full list of author information is available at the end of the article

using VAM when its attachment to the post is loose [11], the deterioration of the timber guardrail crossbeam can be more efficiently assessed without loosening the attachment. In addition, the underground end condition of wooden piles is semi-rigid [16]. The simply supported–simply supported condition has been used to estimate the density in traditional timber buildings using nondestructive tests [17].

The effect of the non-ideal conditions of specimens on VAM should be clarified for applying VAM to the wooden members that are practically used. This matter was examined by changing end conditions of specimens during vibration tests.

Theory

The bending vibrations under the simply supported–simply supported and fixed–fixed conditions are considered. In the case of a thin beam with a constant cross section, the effect of deflections due to shear and rotatory inertia involved in the bending vibrational deflection is negligible, and the Euler–Bernoulli elementary theory of bending can be applied to the bending vibration.

The resonance frequency, which is denoted by f_{n0} (n refers to the resonance mode number and "0" denotes the value without an additional mass), can be expressed as follows:

$$f_{n0} = \frac{1}{2\pi}\left(\frac{m_{n0}}{l}\right)^2\sqrt{\frac{EI}{\rho A}}, \tag{1}$$

where l, E, ρ, I, and A are the span, Young's modulus, density, second moment of area, and cross-sectional area, respectively. m_{n0} is a constant, which is expressed as follows:

$$m_{n0} = n\pi\,(\text{simply supported} - \text{simply supported condition}), \tag{2a}$$

$$\begin{aligned} &m_{10} = 4.730, m_{20} = 7.853, m_{30} = 10.996,\\ &m_{n0} = \frac{1}{2}(2n+1)\pi (n > 3)\\ &(\text{fixed} - \text{fixed condition}). \end{aligned} \tag{2b}$$

The resonance frequency is experimentally reduced by attaching an additional mass while the dimensions, density, and Young's modulus are not altered. Hence, we can state that m_{n0} changes to m_n. Thus, the resonance frequency after attachment of the additional mass is expressed as follows:

$$f_n = \frac{1}{2\pi}\left(\frac{m_n}{l}\right)^2\sqrt{\frac{EI}{\rho A}}. \tag{3}$$

Equations (1) and (3) yield

$$m_n = \sqrt{\frac{f_n}{f_{n0}}}m_{n0}. \tag{4}$$

The frequency equation for the bending vibration with concentrated mass M placed at position $x = al$ (x: distance along the bar, $0 \le a \le 1$, $a + b = 1$) on a bar (Fig. 1) can be expressed as follows:

$$\begin{aligned} &\sin m_n \sinh m_n - \frac{1}{2}\mu m_n(\sinh m_n \sin am_n \sin bm_n\\ &-\sin m_n \sinh am_n \sinh bm_n)\\ &= 0\,(\text{simply supported} - \text{simply supported}), \end{aligned} \tag{5a}$$

[18].

$$\begin{aligned} &(\cos m_n \cosh m_n - 1) - \frac{1}{2}\mu m_n\{(\cos am_n \cosh am_n - 1)\\ &(\sin bm_n \cosh bm_n - \cos bm_n \sinh bm_n)\\ &+(\cos bm_n \cosh bm_n - 1)\\ &(\sin am_n \cosh am_n - \cos am_n \sinh am_n)\} = 0\\ &(\text{fixed} - \text{fixed}), \end{aligned} \tag{5b}$$

where μ is the ratio of the concentrated mass to the mass of the bar and can be defined as follows:

$$\mu = \frac{M}{\rho A l}. \tag{6}$$

To calculate m_n, the measured resonance frequencies (f_{n0} and f_n) are substituted into Eq. (4). Calculated m_n is substituted into Eqs. (5a) and (5b) to calculate μ. The specimen mass and density can be obtained by substituting calculated μ, the concentrated mass, and dimensions of the bar into Eq. (6). The Young's modulus can be calculated by substituting the estimated density, resonance frequency without a concentrated mass, and dimensions of the bar into Eq. (1) [1–5]. The specimen mass is not required in these calculations.

These calculations illustrate the VAM procedure. In the present study, the estimation accuracy of VAM is expressed by the ratio of the specimen mass estimated using VAM (M_{VAM}) to the measured specimen mass (M_0). Here, M_{VAM} represents the product of the estimated mass using the VAM process and length-to-span ratio. The estimation accuracy of VAM in this study is considered to be sufficiently high at $0.9 \le M_{\mathrm{VAM}}/M_0 \le 1.1$.

Materials and methods

Specimens

Sitka spruce (*Picea sitchensis* Carr.) rectangular bars with a width of 25 mm (radial direction, R), heights of 5, 6, 7,

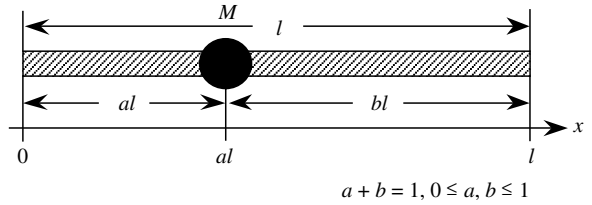

Fig. 1 Beam with an additional mass

8, 9, 10, 11, 12, 13, 14, 15, 16, 17, 18, 19, 20, 21, 22, 23, 24, and 25 mm (tangential direction, T), and a length of 300 mm (longitudinal direction, L) were used as specimens. The surface of each specimen was finished using a tip saw. Three specimens at each dimension were used. The specimens were conditioned at 20 °C and 65% relative humidity until weight became constant. All tests were conducted under the same conditions.

Free–free bending vibration test

To obtain the Young's modulus by bending, free–free flexural vibration tests were conducted according to the following procedure [19]. The test bar was suspended using two threads at the nodal positions of the free–free vibration corresponding to its resonance mode. The bending vibration was initiated by hitting the LR-plane of the specimen at one end using a wooden hammer (hammer head size: 5 mm × 6 mm × 10 mm, 0.85 g), whereas the bar motion was monitored using a microphone (PRECISION SOUND LEVEL METER 2003, NODE Co., Ltd., Tokyo, Japan) at the other end. The signal was processed using a fast Fourier transform (FFT) digital signal analyzer (Multi-Purpose FFT Analyzer CF-5220, Ono-Sokki, Co., Ltd., Yokohama, Japan) to obtain high-resolution resonance frequencies (Fig. 2).

A vibration test was conducted on a specimen without a concentrated mass, and the resonance frequencies in the 1st to 6th modes were measured. Young's modulus (E_{TGH}) and shear modulus of the LT-plane (G_{LT}) were calculated using the Goens–Hearmon regression method based on the Timoshenko theory of bending (TGH method) [20–22]. The Young's modulus in the absence of the effects of shear and rotatory inertia and shear modulus could be obtained using the TGH method for bending vibration.

Bending vibration test under a semi-rigid condition

The bending vibration tests under the semi-rigid condition were conducted according to the following procedure [14]. The apparatus (Takachiho Seiki Co., Ltd., End condition controller KS-200) shown in Fig. 3 was used to provide different end conditions. The 25 mm

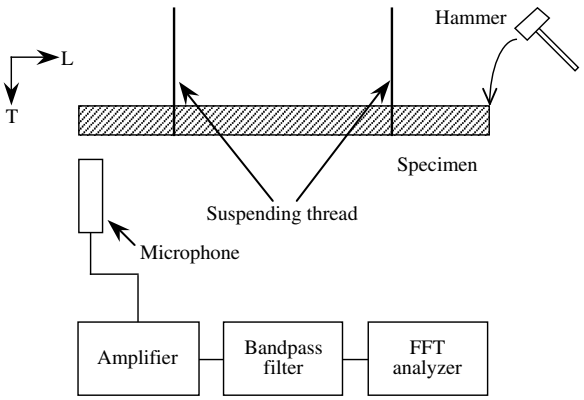

Fig. 2 Schematic diagram of the experimental setup for the free–free bending vibration test

(L) × 25 mm (R) regions from both ends were supported by the posts of the apparatus whose cross section was 25 mm × 25 mm. Consequently, the span was 250 mm. The test bar was compressed by screwing a bolt attached to a load cell. It is thought that the vertical displacement was almost 0 and the rotation was partially restrained at both ends. The compression load was measured by the load cell and recorded using a data logger. Bending vibration was initiated by hitting the LR-plane of the specimen in the vertical direction at the center part using the aforementioned wooden hammer. The bar motion was detected by the aforementioned microphone installed at the center part. The signal was processed using the aforementioned FFT digital signal analyzer to generate high-resolution resonance frequencies. Because the stress relaxation was observed for each set compressive stress, the vibration test was conducted when the load change became sufficiently small.

Vibration tests were conducted on the specimen with and without a steel plate, which was used as the concentrated mass (1.29–7.55 g, as listed in Table 1) and the resonance frequency of the 1st mode was measured. The steel plate was bonded at $x = 0.5\ l$ on the LR-plane using a double-sided tape. The bending vibration test was performed using the same specimen without the concentrated mass during the increase in the compressive stress. After the bending vibration test at maximum compressive stress, which means the stress when loading was stopped in this study, the stress was reduced to 0. Subsequently, the concentrated mass was attached to the same specimen, and the bending vibration test was performed using the same specimen with the concentrated mass during the increase in the

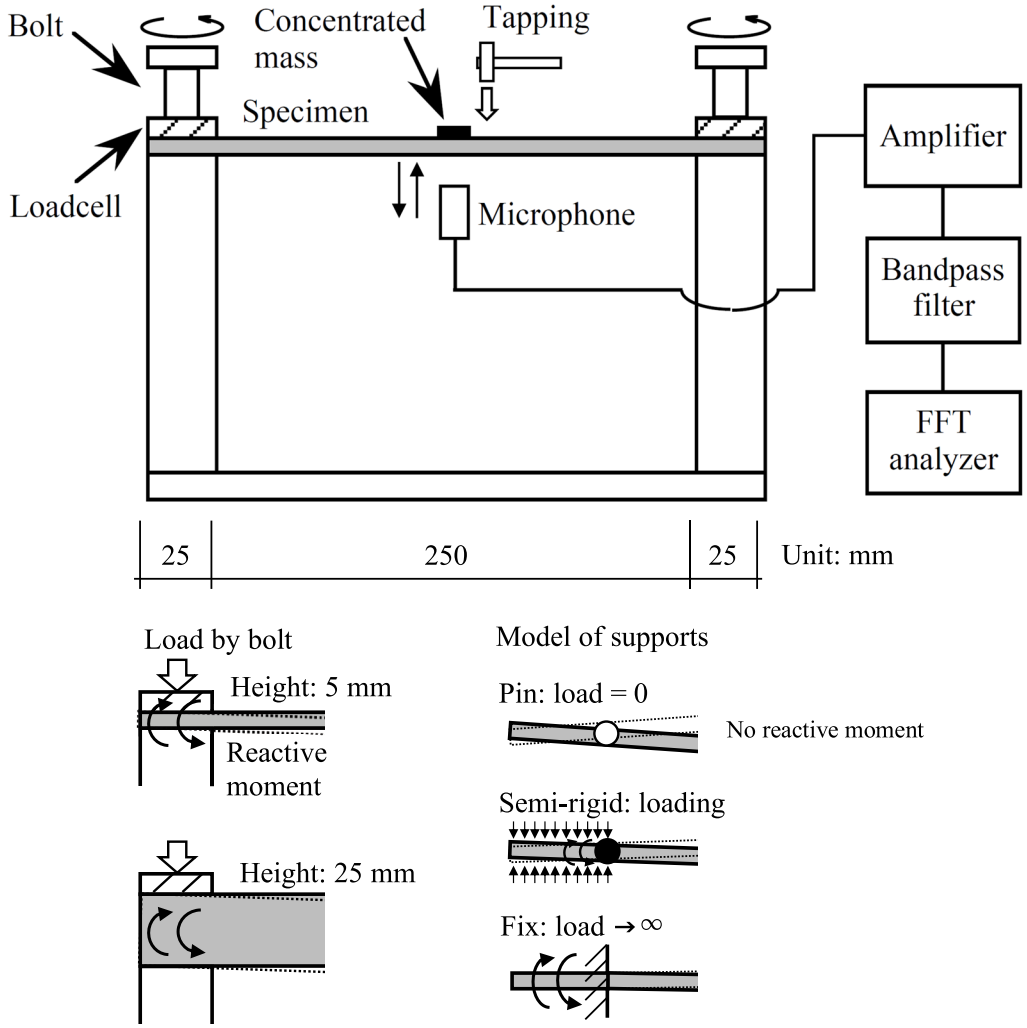

Fig. 3 Schematic diagram of the experimental setup for the bending vibration test under various end conditions

compressive stress. The compressive stress during the resonance frequency measurement with the concentrated mass and that without the concentrated mass were made to have the same value as much as possible.

Results and discussion

The mean and standard deviation of the density were 411 and 26 kg/m^3, respectively, whereas those of the Young's modulus and shear modulus of the LT-plane according to the TGH method were 11.52 and 0.97 GPa, 0.78 and 0.15 GPa, respectively.

Figure 4 shows an example of the changes in the estimation accuracy of VAM during the increase in compressive stress. The changes in M_{VAM}/M_0 were large at the early stage of loading specimens and M_{VAM}/M_0 became stable under the larger compressive stress. Because the compression set caused by the partial compression around the ends of the specimens was observed in the case of specimens with a larger height during the preliminary experiments, the maximum compressive stress for the specimens with a larger height was smaller than that for the specimens with a smaller height.

Figure 5 shows an example of the changes in the measured resonance frequency without the concentrated mass (f_{10M}) during the increase in the compressive stress. The f_{10M} value increased with the increase in compressive stress and approached the value of ideal fixed ends for the 1st resonance mode (f_{FF}) (subscript FF: fixed–fixed). Here, f_{FF} was calculated by introducing E_{TGH} into Eq. (1).

Table 1 Concentrated masses (steel plates) attached to the specimens

Specimen height (mm)	Mass (*g*)	Mass ratio (μ)
5	1.29	0.0896
6	1.91	0.116
7	2.55	0.134
8	2.55	0.118
9	2.55	0.106
10	2.55	0.0951
11	3.84	0.123
12	3.84	0.112
13	3.84	0.104
14	3.84	0.0966
15	5.03	0.141
16	5.03	0.127
17	5.03	0.120
18	5.03	0.113
19	5.03	0.107
20	7.55	0.153
21	7.55	0.146
22	7.55	0.140
23	7.55	0.134
24	7.55	0.128
25	7.55	0.124

Comparing Fig. 4 with Fig. 5, when M_{VAM}/M_0 was stable (larger than 0.5 MPa for height = 5 mm, larger than 1.7 MPa for height = 25 mm), $f_{10\mathrm{M}}$ was stable. In other words, VAM could not be adequately used when the specimen was not properly installed in the apparatus. Hence, M_{VAM}/M_0 at the maximum compressive strength was discussed hereafter.

Because $f_{10\mathrm{M}}$ was close to f_{FF} and was less than f_{FF} in the case of the specimen with a smaller height as shown in Fig. 5, the end condition was considered as an imperfect fixed condition in this study. Hence, the frequency equation under the fixed–fixed end condition, i.e., Eq. (5b) was used to estimate the specimen mass by VAM hereafter.

According to Fig. 6, M_{VAM}/M_0 increased with the increase in the specimen height (h), i.e., greatly deviated from 1 in the specimens with a larger height. The M_{VAM}/M_0 value was experimentally approximated as follows:

$$\frac{M_{\mathrm{VAM}}}{M_0} = 0.0078927h^2 - 0.095749h + 1.3336 \quad (\text{coefficient of determination} = 0.98395). \tag{7}$$

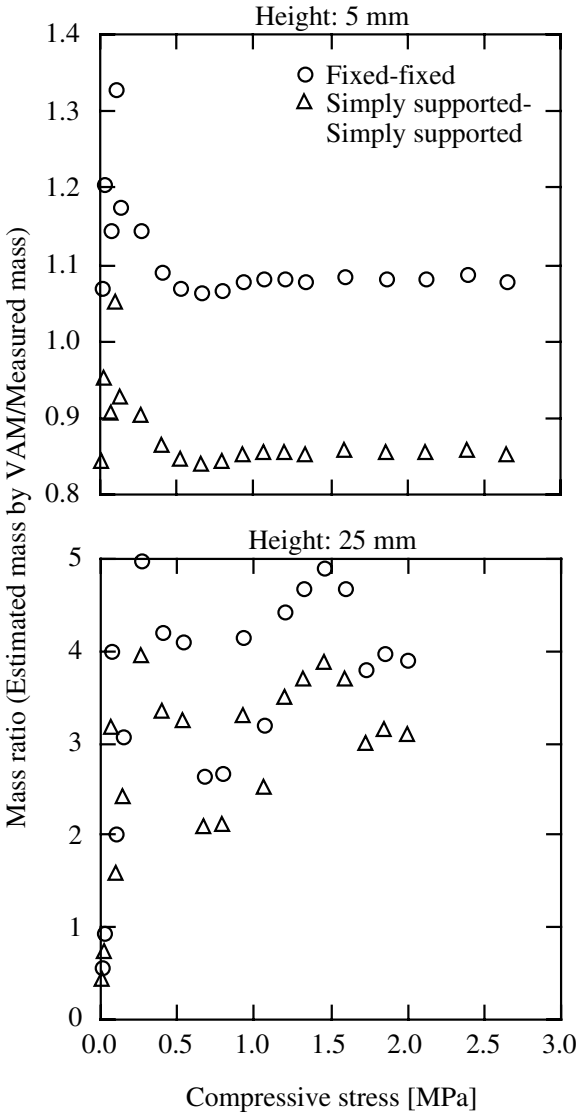

Fig. 4 Example of the changes in the estimation accuracy of VAM during the increase in compressive stress

We assume that the increase in M_{VAM}/M_0 shown in Fig. 6 is related to the result of $f_{10\mathrm{M}} < f_{\mathrm{FF}}$ shown in Fig. 5. It is thought that $f_{10\mathrm{M}} < f_{\mathrm{FF}}$ was caused by the deflections due to shear and rotatory inertia involved in the apparent deflection in the bending vibration [20] and semi-rigid condition.

The frequency equation taking into account the effects of shear and rotatory inertia under the fixed–fixed condition for a rectangular bar without the concentrated mass is expressed by Eq. (8) based on the boundary condition [23]:

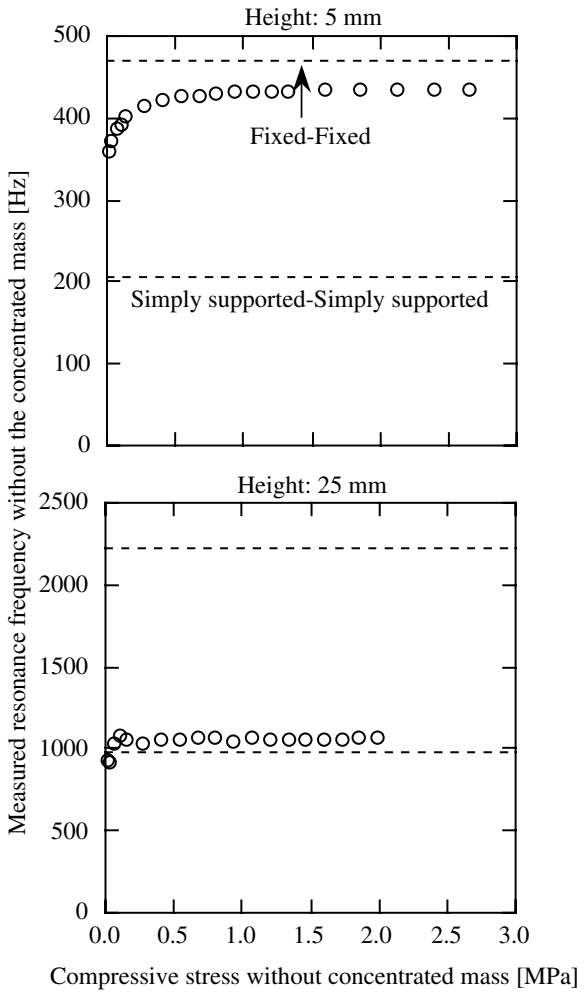

Fig. 5 Example of the changes in the measured resonance frequency without the concentrated mass during the increase in compressive stress

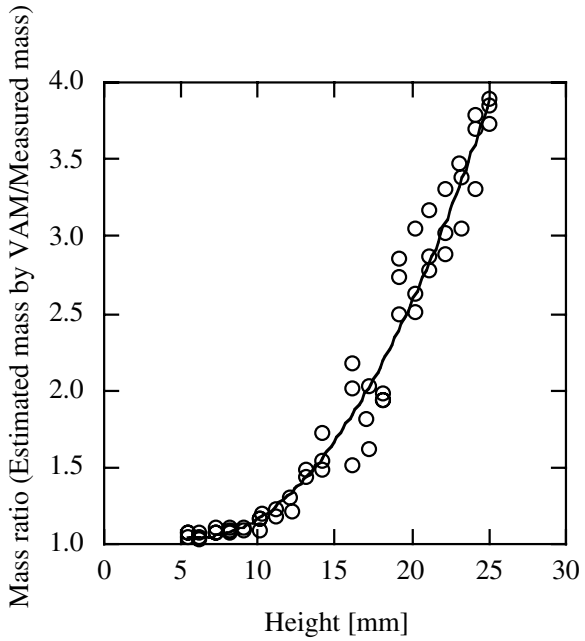

Fig. 6 Change in the mass ratio (estimated specimen mass by VAM/measured specimen mass) that indicates the estimation accuracy of VAM with respect to the specimen height

$$2(\cos\beta k_{n0}\cosh\beta k_{n0}-1)+\left(\frac{\alpha\eta}{\beta\varepsilon}-\frac{\beta\varepsilon}{\alpha\eta}\right)\sin\beta k_{n0}\sinh\beta k_{n0}=0, \tag{8}$$

$$\alpha=\sqrt{\sqrt{B_t^2k_{n0}^4+1}-A_tk_{n0}^2}, \tag{9}$$

$$\beta=\sqrt{\sqrt{B_t^2k_{n0}^4+1}+A_tk_{n0}^2}, \tag{10}$$

$$\varepsilon=\sqrt{B_t^2k_{n0}^4+1}+B_tk_{n0}^2, \tag{11}$$

$$\eta=\sqrt{B_t^2k_{n0}^4+1}-B_tk_{n0}^2, \tag{12}$$

$$A_t=\frac{I}{2Al^2}\left(\frac{sE}{G}+1\right), \tag{13}$$

$$B_t=\frac{I}{2Al^2}\left(\frac{sE}{G}-1\right). \tag{14}$$

k_n and s are a constant and shear factor (=1.2 for rectangular cross section). Substituting the measured E_{TGH}, G_{LT} and l/h into Eq. (8), k_n can be obtained. Mathematica 10.4J software (Wolfram Research Co., Ltd.) was used in the calculation. The relationship of Eq. (15) exists.

$$f_{n0SR}=\frac{1}{2\pi}\left(\frac{k_{n0}}{l}\right)^2\sqrt{\frac{EI}{\rho A}}\ (\text{subscript SR : shear and rotatory inertia}). \tag{15}$$

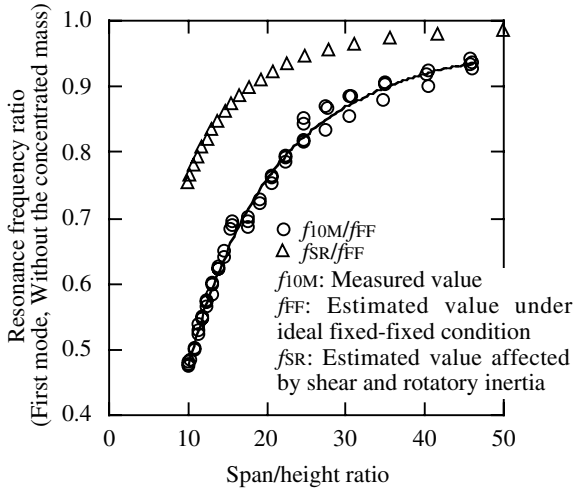

Fig. 7 Change in the frequency ratio without the concentrated mass with respect to the span-to-height ratio

From Eqs. (1) and (15),

$$\frac{f_{n0SR}}{f_{FF}} = \left(\frac{k_{n0}}{m_{n0}}\right)^2. \tag{16}$$

The frequency ratios of f_{10SR}/f_{FF} and f_{10M}/f_{FF} were plotted against l/h in Fig. 7. The f_{10M}/f_{FF} value was smaller than f_{10SR}/f_{FF}. It is thought that the difference between f_{10SR}/f_{FF} and f_{10M}/f_{FF} were caused by the semi-rigid condition at the end. The difference increased with the decrease in l/h.

In the previous study, M_{VAM}/M_0 decreased with the decrease in l/h under the free–free condition [10] while the opposite tendency is observed in Fig. 6. We think that semi-rigid condition more strongly affected M_{VAM}/M_0 rather than the effects due to shear and rotatory inertia.

The M_{VAM}/M_0 value that was larger than 1 was discussed. The VAM procedure expressed by Eqs. (1)–(5) are based on the assumption that a specimen is under the ideal conditions, however, the measured resonance frequencies with and without the concentrated mass subjected to the effect of the non-ideal condition (f_{1M}, f_{10M}) were used as f_1 and f_{10} for VAM (Eq. (4)), respectively, in the "Results and discussion" Section. Because $m_{10}=4.73$ for the ideal condition was substituted into Eq. (4), the resonance frequency ratio f_{1M}/f_{10M} was discussed.

The relationship between f_n/f_{n0} and f_{nM}/f_{n0M} was experimentally investigated. Ideal m_n/m_{n0} could be calculated by substituting the measured mass ratio = (measured concentrated mass)/(measured specimen mass) into Eq. (5b). Mathematica 10.4J software was used in the calculation. By substituting the obtained m_n/m_{n0} into Eq. (4), ideal f_n/f_{n0} can be calculated.

Here, degree of ideality (DI) was defined as:

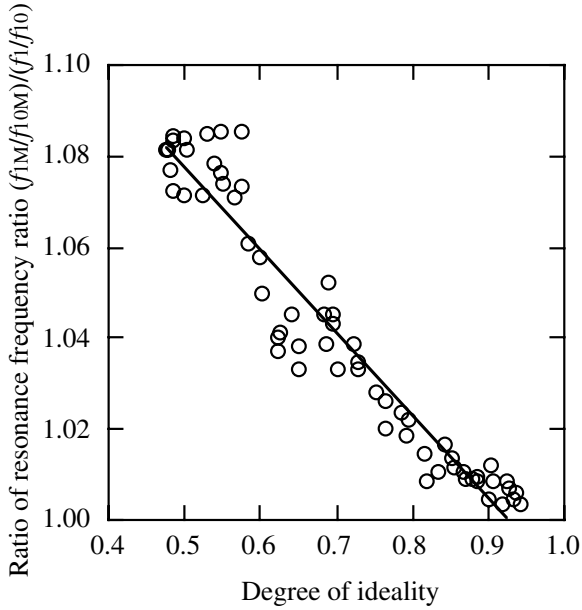

Fig. 8 Change in the frequency ratio (measured value/theoretical value) with respect to the degree of ideality

$$DI = \frac{f_{10M}}{f_{FF}} (\leq 1), \tag{17}$$

where $DI=1$ indicates the ideal condition of specimens and $DI<1$ indicates that a specimen deviates from the ideal condition. According to Fig. 7, DI was experimentally approximated as follows:

$$DI = -3.9223 \times 10^{-7}\left(\frac{l}{h}\right)^4 + 5.837 \times 10^{-5}\left(\frac{l}{h}\right)^3 - 0.0033909\left(\frac{l}{h}\right)^2 + 0.095073\frac{l}{h} - 0.18954 \quad (\text{coefficient of determination} = 0.99639). \tag{18}$$

The ratio $(f_{1M}/f_{10M})/(f_1/f_{10})$ was plotted against DI (Fig. 8), and a liner relationship existed at 1% significance level as follows:

$$\frac{f_{1M}/f_{10M}}{f_1/f_{10}} = -0.1806DI + 1.1675 \quad (\text{correlation coefficient} = 0.96386). \tag{19}$$

Since $f_{1M}/f_{10M} > f_1/f_{10}$ as shown in Fig. 8, m_1 obtained by substituting f_{1M}/f_{10M} into Eq. (4) was larger than m_1 under the ideal condition. According to the previous study [4], m_n theoretically decreases with the increase in μ under the fixed–fixed condition. The M_{VAM} value increases with the decrease in μ from Eq. (6). Therefore,

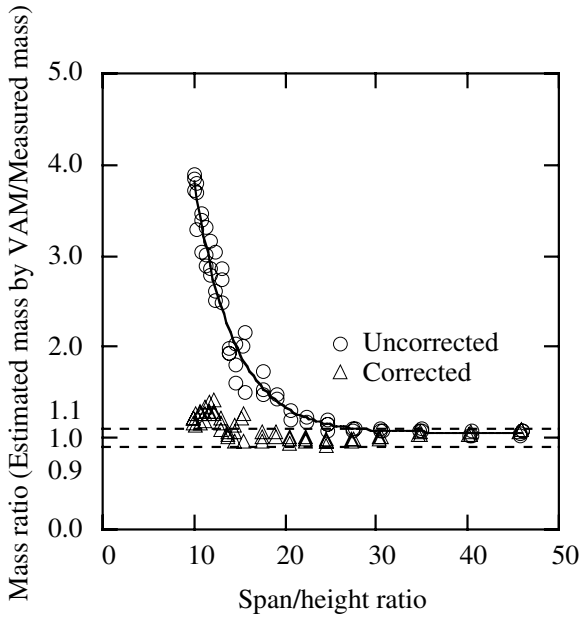

Fig. 9 Corrected mass ratio (estimated specimen mass by VAM/measured specimen mass) at various span-to-height ratios

M_{VAM}/M_0 under the non-ideal condition was larger than that under the ideal condition.

The M_{VAM} value could be corrected by according to the following procedure. Measured *l/h* was substituted into Eq. (18) to estimate *DI*. Substitution of the estimated *DI* and the measured f_{1M} and f_{10M} into Eq. (19) yielded the estimation of f_1/f_{10}. The m_1 value was estimated by substituting the estimated f_1/f_{10} and $m_{10}=4.73$ into Eq. (4). The μ value was estimated by substituting the estimated m_1 and the position of the concentrated mass into Eq. (5b). The M_{VAM} value was corrected with the substitution of the estimated μ into Eq. (6). The corrected M_{VAM}/M_0 is shown in Fig. 9. Many results could be improved using this correction method.

Conclusions

VAM was applied to small clear specimens under conditions where wooden members are expected to be practically used, and the following results were obtained:

1. VAM could not be adequately used when the specimen was not properly installed in the apparatus.
2. Because f_{10M} was close to f_{FF} and was less than f_{FF} in the case of the specimen with a smaller height, the end condition at the maximum stress was considered as an imperfect fixed condition in this study.
3. M_{VAM}/M_0 increased with the increase in the specimen height and greatly deviated from 1 in specimen with a larger height.
4. The deviation in M_{VAM}/M_0 from 1 was due to the substitution of the measured resonance frequencies into the frequency equation that required the resonance frequencies under the ideal fixed–fixed condition.
5. A correction method for M_{VAM}/M_0 was subsequently proposed.

Abbreviations

VAM: Vibration method with additional mass; L: Longitudinal direction; R: Radial direction; T: Tangential direction; FFT: Fast Fourier transform.

Acknowledgements

This study was supported by Research grant #201805 of the Forestry and Forest Products Research Institute and JSPS KAKENHI Grant Number JP20H03052.

Author contributions

All authors designed the experiments. YK performed the experiments, analyzed the data, and was a major contributor in writing the manuscript. All authors contributed to interpretation and discussed results. All the authors read and approved the final manuscript.

Funding

This study was supported by Research grant #201805 of the Forestry and Forest Products Research Institute and JSPS KAKENHI Grant Number JP20H03052.

Availability of data and materials

All data generated or analyzed during this study are included in this published article.

Declarations

Competing interests

The authors declare that they have no competing interests.

Author details

[1]Forestry and Forest Products Research Institute, 1 Matsunosato, Tsukuba, Ibaraki 305-8687, Japan. [2]Polytechnic University, 2-32-1 Ogawa-nishimachi, Kodaira-shi, Tokyo 187-0035, Japan.

Received: 2 April 2022 Accepted: 15 June 2022
Published online: 28 June 2022

References

1. Skrinar M (2002) On elastic beams parameter identification using eigenfrequencies changes and the method of added mass. Comput Mater Sci 25:207–217
2. Türker T, Bayraktar A (2008) Structural parameter identification of fixed end beams by inverse method using measured natural frequencies. Shock Vib 15:505–515
3. Matsubara M, Aono A, Kawamura S (2015) Experimental identification of structural properties of elastic beam with homogeneous and uniform cross section. Trans JSME. https://doi.org/10.1299/transjsme.15-00279
4. Kubojima Y, Kato H, Tonosaki M, Sonoda S (2016) Measuring Young's modulus of a wooden bar using flexural vibration without measuring its weight. BioRes 11:800–810

5. Matsubara M, Aono A, Ise T, Kawamura S (2016) Study on identification method of line density of the elastic beam under unknown boundary conditions. Trans JSME. https://doi.org/10.1299/transjsme.15-00669
6. Sonoda S, Kubojima Y, Kato H (2016) Practical techniques for the vibration method with additional mass Part 2: Experimental study on the additional mass in longitudinal vibration test for timber measurement. In: Proceedings of the World Conference on Timber Engineering (WCTE 2016), Vienna, August 22–25, 2016
7. Kubojima Y, Sonoda S, Kato H (2017) Practical techniques for the vibration method with additional mass: effect of crossers' position in longitudinal vibration. J Wood Sci 63:147–153
8. Kubojima Y, Sonoda S, Kato H (2017) Practical techniques for the vibration method with additional mass: effect of specimen moisture content. J Wood Sci 63:568–574
9. Kubojima Y, Sonoda S, Kato H (2018) Practical techniques for the vibration method with additional mass: bending vibration generated by tapping cross section. J Wood Sci 64:16–22
10. Kubojima Y, Sonoda S, Kato H, Harada M (2020) Effect of shear and rotatory inertia on the bending vibration method without weighing specimens. J Wood Sci 66:51
11. Kubojima Y, Sonoda S, Kato H (2018) Application of the vibration method with additional mass to timber guardrail beams. J Wood Sci 64:767–775
12. Kubojima Y, Sonoda S, Kato H (2020) Mass of piled lumber estimated through vibration test. J Wood Sci 66:32
13. Kubojima Y, Sonoda S, Kato H (2021) Mass of piled round bar estimated through vibration tests. Wood Fib Sci 53:216–227
14. Kubojima Y, Ohsaki H, Kato H, Tonosaki M (2006) Fixed-fixed flexural vibration testing method of beams for timber guardrails. J Wood Sci 52:202–207
15. Kubojima Y, Kato H, Tonosaki M (2012) Fixed-fixed flexural vibration testing method of actual-size bars for timber guardrails. J Wood Sci 58:211–215
16. Kubojima Y, Kato H, Hara T, Sonoda S (2022) Vibration and its application of wooden pile in the ground. Part 4. Underground end condition for wooden piles one year after construction. In: Programs of the 72nd Annual Meeting of the Japan Wood Research Society, C15-P-13, Nagoya-Gifu, March 15–17, 2022
17. Oida A, Ishida T, Sugino M, Hayashi Y (2021) Study on estimating density in traditional timber buildings by non-destructive test. AIJ J Technol Des 27:708–713
18. Taniguchi O (1968) Mechanical Vibration. Corona publishing CO., LTD, Tokyo, pp 165–166
19. Kubojima Y, Yoshihara H, Ohta M, Okano T (1996) Examination of the method of measuring the shear modulus of wood based on the Timoshenko theory of bending. Mokuzai Gakkaishi 42:1170–1176
20. Timoshenko SP (1921) On the correction for shear of the differential equation for transverse vibrations of prismatic bars. Phil Mag 41(245):744–746
21. Goens E (1931) Über die Bestimmung des Elastizitätsmodulus von Stäben mit Hilfe von Biegungsschwingungen. Annal Phys 403(6):649–678
22. Hearmon RFS (1958) The influence of shear and rotatory inertia on the free flexural vibration of wooden beams. Brit J Appl Phys 9(10):381–388
23. Komatsu K, Toda S (1977) Beam-type vibrations of short thin cylindrical shells. Tech Rep Natl Aerosp Lab 502:1–11

Publisher's Note